

---

# Exclusivity graph approach to Instrumental inequalities

---

## Abstract

Instrumental variables allow the estimation of cause and effect relations even in presence of unobserved latent factors, thus providing a powerful tool for any science wherein causal inference plays an important role. More recently, the instrumental scenario has also attracted increasing attention in quantum physics, since it is related to the seminal Bell's theorem and in fact allows the detection of even stronger quantum effects, thus enhancing our current capabilities to process information and becoming a valuable tool in quantum cryptography. In this work, we further explore this bridge between causality and quantum theory and apply a technique, originally developed in the field of quantum foundations, to express the constraints implied by causal relations in the language of graph theory. This new approach can be applied to any causal model containing a latent variable. Here, by focusing on the instrumental scenario, it allows us to easily reproduce known results as well as obtain new ones and gain new insights on the connections and differences between the instrumental and the Bell scenarios.

## Introduction

Inferring whether a variable  $A$  is the cause of another variable  $B$  is at the core of causal inference. However, unless interventions are available [1], one cannot exclude that observed correlations between  $A$  and  $B$  are due to a latent common factor, thus hindering any causal conclusions. To cope with that, instrumental variables (IV) have been introduced [2, 3]. Under the assumption that they are independent of any latent common factors,

IV can be used to put non-trivial bounds on the causal effect between  $A$  and  $B$ . To this aim, first, one has to guarantee that an appropriate instrument (fulfilling a set of causal constraints) has been employed, precisely the goal of the so-called instrumental tests [2, 3]. Their violation, at least in classical physics, is an unambiguous proof that some of the causal assumptions underlying the instrumental causal structure are not fulfilled, that is, one should identify and use another instrumental variable.

The first instrumental tests have been introduced by Pearl [2], in the form of inequalities providing a necessary condition for a given observed probability distribution to be compatible with the instrumental causal structure. Following that, Bonet [3] introduced a general framework, showing that the instrumental correlations define a polytope, a convex set from which the non-trivial boundaries are precisely the instrumental inequalities. Bonet's framework allows for the derivation of new inequalities as well as proving general results, for instance, the fact that if variable  $A$  is continuous, no instrumental test exists. However, two main drawbacks are presented. First, the systematic derivation of new inequalities quickly becomes unfeasible as the variables' cardinality increases. Second, as recently shown, in quantum physics, violations of the instrumental tests are possible even though the whole process is indeed subjected to an instrumental causal structure [4, 5]. In the quantum case, instrumentality violations witness the presence of quantum entanglement as the latent factor and prove a stronger form of quantum non-locality compared to the famous Bell's theorem [4]. As a consequence, typical bounds on the causal influence of  $A$  into  $B$  have to be reevaluated and reinterpreted in the presence of quantum effects [1].

Our aim in this paper is to provide a novel and complementary framework to the analysis of instrumental tests and that addresses the two drawbacks mentioned above. The proposed method is based on a graph theoretical approach introduced in the foundations of quantum physics to analyze the possible correlations obtained in quantum

experiments [1]. This method allow us to reproduce the classical results by Bonet and to straightforwardly generalize them in the quantum scenario. It also offers an easy way to check for the presence of a gap between the quantum and classical case, for any causal scenario involving a single latent variable.

The paper is organized as follows: firstly we provide an introduction about the instrumental scenario, both from a classical perspective, as well as its quantum violations, and about the exclusivity graph approach. Then, we show a novel application of this approach to the field of causal inference. Indeed, it is possible to exploit these graphs in order to obtain inequality constraints, as we show in particular for the instrumental scenario, in the case where the two parties can respectively choose among four and three 3-outcome measurements.

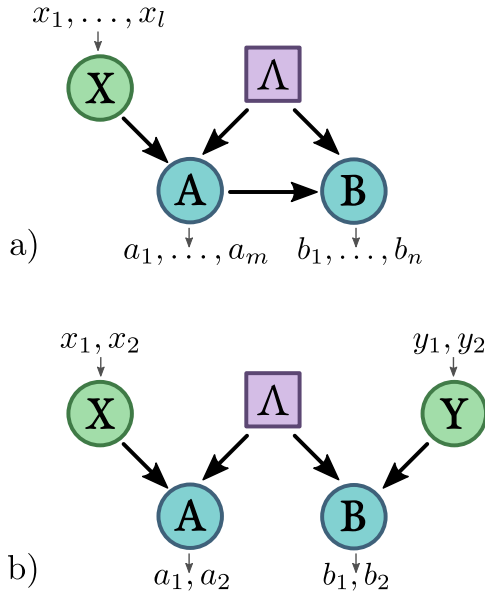


Figure 1: Directed acyclic graph (DAG) representation for **a)** a general Instrumental scenario, with  $l$  possible values for the random variable  $X$  and  $m, n$  possible outcomes for  $A$  and  $B$  respectively, and for **b)** the CHSH scenario where all the variables  $X, Y, A$  and  $B$  can only take two possible values.

## Instrumental variables, estimation of causal influences and a new form of quantum non-locality

It has become standard to represent causal relations via directed acyclic graphs (DAG), where the nodes represent random variables interconnected by directed edges (arrows) accounting for their cause and effect relations [1]. A set of variables  $(X_1, \dots, X_n)$  form a Bayesian

network with respect to the graph if every variable  $X_i$  can be expressed as a function of its parents  $PA_i$  and potentially an unobserved noise term  $U_i$ , such that  $U_i$  are jointly independent. This implies that the probability distribution of such variables should have a Markov decomposition<sup>1</sup>

$$p(x_1, \dots, x_n) = \prod_{i=1}^n p(x_i | pa_i). \quad (1)$$

Importantly, a DAG typically implies non-trivial constraints over the probability distributions that are compatible with it. That is, simply from observational data and without the need of interventions, one can test whether some observed correlations are incompatible with some causal hypothesis.

Within this context, an important DAG is that corresponding to the instrumental scenario (see Fig.1-a). Following the Markov decomposition, any empirical data encoded in the probability distribution  $p(a, b|x)$  and compatible with the instrumental causal structure can be decomposed as

$$p(a, b|x) = \sum_{\lambda} p(a|x, \lambda) p(b|a, \lambda) p(\lambda). \quad (2)$$

Two causal assumptions are employed to arrive at the decomposition above. First, the assumption that  $p(x, \lambda) = p(x)p(\lambda)$ , which implies the independence of the instrument and the common ancestor. Second, the assumption that even though  $X$  and  $B$  can be correlated, all these correlations are mediated by  $A$ . In other terms, there is no direct causal influence between  $X$  and  $B$  and  $p(b|x, a, \lambda) = p(b|a, \lambda)$ .

The instrumental variables have been originally introduced to estimate parameters in econometric models of supply and demand [6] and, since then, have found a wide range of applications in various other fields [7, 8]. To illustrate its power, consider that variables  $A$  and  $B$  are related by a simple structural equation  $B = \gamma A + \Lambda$ , where  $\Lambda$  may represent a latent common factor. By assumption, the instrumental variable  $X$  should be independent of  $\Lambda$ , thus implying that the causal strength can be estimated as  $\gamma = \text{Cov}(X, B) / \text{Cov}(X, A)$  where  $\text{Cov}(X, A) = \langle X, A \rangle - \langle X \rangle \langle A \rangle$  is the covariance between  $X$  and  $A$ . Strikingly, one can estimate the causal strength even without any information about the latent factor  $\Lambda$ . More generally and without assumptions about the functional dependence among the variables, the empirical data encoded in the probability distribution

<sup>1</sup>Uppercase letters label variables and lowercase label the values taken by them, for instance,  $p(X_i = x_i, X_j = x_j) \equiv p(x_i, x_j)$ .

$p(a, b|x)$  can also be used to bound different quantifiers of causality between  $A$  and  $B$  [].

Clearly, however, to draw any causal conclusions, first it is necessary to certify that one has a valid instrument. This is achieved via instrumental inequalities, first introduced by Pearl [?]. If we allow the variables  $X, A, B$  to take the values in the range  $x = 1, \dots, l, a = 1, \dots, m$  and  $b = 1, \dots, n$  Pearl showed that the instrumental causal structure implies that

$$\sum_{j=0}^n P(a_i b_j | x_{k(i,j)}) \leq 1, \quad (3)$$

for all  $i \in 1, \dots, m$  and for all the possible functions  $k(i, j)$  where  $p(a = i, b = j | x = k) = p(a_i, b_j | x_k)$ .

Extending these results, Bonet [3] provided a general geometric framework for the derivation of instrumental inequalities. Instrumental correlations define a convex set, a polytope described by finitely many extremal points, or alternatively by a finite number of facets, among which, the non-trivial are precisely the instrumental inequalities. In particular, considering the case  $(l, m, n) = (3, 2, 2)$ , it was proven that there are two inequivalent classes of instrumental inequalities (those not obtained from each other by permuting the labels of  $a_i, b_j$  and  $x_k$ ). One class corresponding to Pearl's inequality (3) and the other given by

$$P(a_1 b_1 | x_1) + P(a_2 b_2 | x_1) + P(a_1 b_1 | x_2) + P(a_2 b_1 | x_2) + P(a_1 b_2 | x_3) \leq 2. \quad (4)$$

All these conclusions and results, however, rely on a classical description of causal and effect relations, that since Bell's theorem [] we know do not apply to the world governed by quantum mechanics. This has motivated the question of whether many of the cornerstones in causal inference have to be reevaluated or reinterpreted in the presence of quantum effects []. Indeed, as recently shown [4], violations of the instrumental tests are possible even though the causal constraints underlying the instrumental scenario are fulfilled. As shown in the experimental implementation of the instrumental test [4], this is possible due to the presence of quantum entanglement acting as latent common ancestor. Considering an entangled sources of photons, an alternative version of Bonet's inequality (written in terms of expectation values, upper bounded by 3, in the classical realm) has been tested, implying a violation of the inequality (4) with a value of  $3.258 \pm 0.020$ .

Altogether, this shows the necessity of a new unifying framework, not only considering what are the classical instrumental correlations but as well the ones achievable

if the underlying latent factor might have a quantum origin. In the following we will achieve that by proposing a graph-theoretical approach to analyze the instrumental inequalities.

## The exclusivity graph approach

The graph-theoretical approach we propose here, was initially developed for the study of non-contextual inequalities [9] as well as Bell non-locality scenarios [?]. In this formalism, every possible event, i.e. every possible set of measurement outcomes  $a_1, \dots, a_n$  corresponding to given measurement settings  $x_1, \dots, x_n$  (each of which can be understood as an instrument), is associated to a vertex in a (undirected) graph  $G = (V, E)$ . Two vertices  $u, v \in V$  are then connected by an edge  $uv \in E$  if and only if they are exclusive, i.e. if exists a measurement/instrument that can distinguish between them. Any linear constraint (like the instrumental inequalities) can be expressed defining a linear function

$$I_w(p) = \sum_{\substack{a_1, \dots, a_n \\ x_1, \dots, x_n}} w_{a_1, \dots, a_n} p(a_1, \dots, a_n | x_1, \dots, x_n) \quad (5)$$

on the probabilities of possible events. This linear function can be represented by the weighted exclusivity graph  $G$ . Nicely, as it will be discussed below, bounds for the maximum values for  $I_w(p)$  achievable in classical and quantum physical theories can be related to two well-known graph invariants []: the independence number  $\alpha(G, w)$  and the Lovász theta  $\theta(G, w)$ , respectively. In the following, we will briefly introduce these concepts and their interconnections, a more extensive and detailed account can be found in [9, 10, ?]

Consider a graph  $G(V, E)$  with vertex weights  $w$ , and  $|V| = n$ . We call a *characteristic labelling* for  $U \subseteq V$  a vector  $x_v \in \{0, 1\}^n$  such that  $x_v = 1$  if  $v \in U$  and  $x_v = 0$  otherwise.

An *independent set* or *stable set* is a set  $S \subset V$  such that  $uv \notin E$  for all  $u, v \in S$ . The independence number  $\alpha(G, w)$  is defined as the maximum number of vertices (weighted with  $w$ ) of an independent set of  $G$ . Is also customary to define the set  $\text{STAB}(G)$  as the convex hull of all the characteristic labellings of stable sets:

$$\text{STAB}(G) = \{x : x \text{ is a stable labelling of } G\}. \quad (6)$$

Using this definition the independence number becomes:

$$\alpha(G, w) = \max\{w \cdot x : x \in \text{STAB}(G)\} \quad (7)$$

From these definitions, we can see that  $\alpha(G, w)$  corresponds to the classical bound of the inequality, since it is exactly the maximum over the convex set defined by

all the deterministic strategies respecting the exclusivity constraints.

We now call an *orthonormal labelling* of dimension  $d$  a map  $a_v : V \rightarrow \mathbb{R}^d$  such that  $a_v \cdot a_u = 0$  for all  $uv \in E$  and  $|a_v|^2 = 1$ , and we define the set  $\text{TH}(G)$  as:

$$\text{TH}(G) = \{x : x_v = (a_v)_1 \text{ where } a_v \text{ is an orthonormal labelling of } G\} \quad (8)$$

It can be proved that this set includes all correlations permitted by quantum theory<sup>2</sup>, but in general is larger as it contains correlations beyond those achieved by quantum mechanics [?]. Maximizing over  $\text{TH}(G)$  gives the Lovász theta:

$$\theta(G, w) = \max\{w \cdot x : x \in \text{TH}(G)\} \quad (9)$$

which upper-bounds the maximum quantum value. This approach provides a useful condition to check if a given graph  $G$  admits a quantum violation. Indeed it can be proven that  $\text{TH}(G) = \text{STAB}(G)$  if and only if  $G$  does not contain a cycle  $C_n$  with  $n \geq 5$  and odd, or its complement as an induced subgraph. This follows directly from the notorious “sandwich theorem” [?, 14] and the “strong perfect graph theorem” [15]. The first one states that the number  $\theta(G)$  is always “sandwiched” between the independence number of the graph  $\alpha(G)$  and another quantity called the *chromatic number*  $\chi(G)$ , i.e. the smaller number of colors needed to label the vertices such that vertices connected by an edge always have different colors.

$$\alpha(G) \leq \theta(G) \leq \chi(G) \quad (10)$$

When equality holds in equation (10) for a graph  $G$  and all its induced subgraphs,  $G$  is called *perfect*. For perfect graph we can definitely exclude the existence of a quantum violation, since  $\alpha(G) = \theta(G)$ . The second theorem then gives a useful condition to check if a graph is perfect or not. In particular it affirms that a graph  $G$  is perfect if and only if it does not contain a  $n$ -cycle graph with  $n \geq 5$  and odd or its complement as an induced subgraph.

Besides signaling the presence of a possible quantum violation of classical constraint, induced cycle subgraphs are also experimentally interesting because they give the simplest inequalities (in terms of number of probabilities to estimate), to test this violation.

## 1 Exclusivity graph method applied to causal models

Next we show how the techniques presented in the previous section can be employed to analyze a broad class of

<sup>2</sup>As proved in [?] this set corresponds to the level  $1 + AB$  of the NPA (Navascués-Pironio-Acín) hierarchy [13].

causal models. Consider the DAG depicted in fig 2, with  $k$  observable variables  $A_k$  with potential causal arrows among them,  $l$  instruments  $X_l$  with no incoming edges, and a single unobservable latent variable  $\Lambda$  acting as a potential common factor for all  $A_k$  (but not to  $X_l$ ).

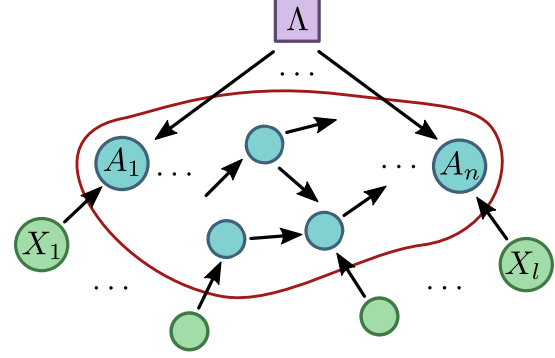


Figure 2: Representation of the class of causal structures to which our method can be applied, which are those with  $k$  observable variables,  $l$  instruments and a single latent variable.

A *non-exclusivity* graph can be associated with such a DAG as follows:

- Nodes are associated to events like  $a|x$ , where  $a = (a_1, \dots, a_k)$  and  $x = (x_1, \dots, x_l)$ .
- Two nodes  $a|x$  and  $a'|x'$  are linked by an edge if and only if
  1. for all  $i, j \in \{1, \dots, k\}$  if  $A_i \rightarrow A_j$  then  $\exists g_{ij} : g_{ij}(a_i) = a_j$  and  $g_{ij}(a'_i) = a'_j$ .
  2. for all  $i \in \{1, \dots, l\}$  and  $j \in \{1, \dots, k\}$  if  $X_i \rightarrow A_j$  then  $\exists f_{ij} : f_{ij}(x_i) = a_j$  and  $f_{ij}(x'_i) = a'_j$ .

As we will show next, considering the particular case of the instrumental scenario [], one can apply the graph-theoretical methods delineated before to the complement of this graph,  $G = \bar{G}$ , and its subgraphs. This allows to obtain instrumental inequalities and their respective quantum and classical bounds.

### 1.1 The Instrumental exclusivity graph

As a first application we will restrict our attention to the case of dichotomic observables ( $n = m = 2$ ), considering  $p(ab|x)$  with  $a, b \in \mathcal{A} = \mathcal{B} = \{0, 1\}$  and  $x \in \mathcal{X} = \{0, \dots, l\}$ , the probability of having outcomes  $a$  and  $b$  with the instrument assuming the value  $x$ . As detailed above, the non-exclusivity graph for the instrumental scenario is obtained by linking two events  $ab|x$

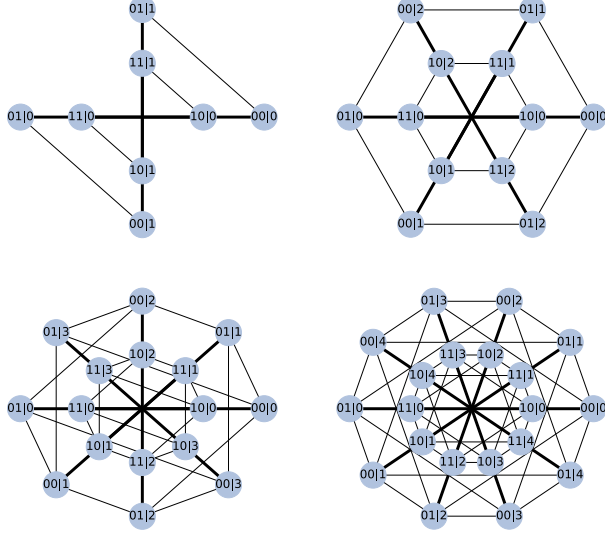


Figure 3: The exclusivity graph for the instrumental scenario  $l22$  with  $l = 2, 3, 4, 5$  respectively from top left to bottom right. To simplify the representation cliques are represented with the bold lines in the figure.

and  $a'b'|x'$  if there exist two functions  $f : \mathcal{X} \rightarrow \mathcal{A}$  and  $g : \mathcal{A} \rightarrow \mathcal{B}$  such that:

$$\begin{aligned} a &= f(x) \quad \text{and} \quad a' = f(x') \\ b &= g(a) \quad \text{and} \quad b' = g(a') \end{aligned} \quad (11)$$

As shown in Fig. 3, we construct the exclusivity graphs for various  $l$  and use the methods described earlier to obtain the classical and quantum bounds for several inequalities in the instrumental scenario.

First, consider the case  $l = 2$ , for which Pearl's inequality (3) defines the only instrumental inequality. It has been shown that this inequality does not have a quantum violation [1]. For that, general probabilistic Bayesian networks, including classical and quantum causal models as particular cases, had to be introduced. In contrast, in our method it is straightforward not only to derive the classical bound to Pearl's inequality but also show that there is no quantum violation of the inequality. Indeed in the case of  $l = 2$  inequalities (3) becomes:

$$P(a0|x_1) + P(a1|x_2) \leq 1 \quad (12)$$

which are just the classical constraint given by the exclusivity conditions, represented by the edges of the graph (see Fig. 3). The fact that no quantum violation is allowed instead follows immediately from the fact that the corresponding exclusivity graph (and its complement) does not contain any odd cycle or anticyle with more than 5 vertices, which makes it a perfect graph, i.e.  $TH(G) = STAB(G)$ . This can be easily generalized to any number of output  $n, m$  as shown in the methods section. In

this way we can exclude the presence of any quantum violation for any instrumental scenario with  $l = 2$  and an arbitrary number of outputs.

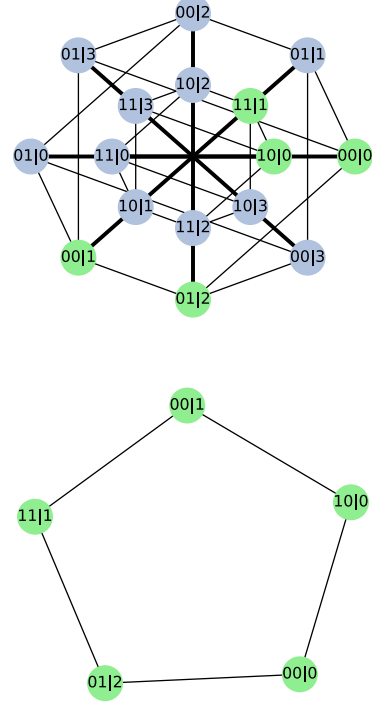


Figure 4: The exclusivity graph of the Bonet inequality, as an induced subgraph of complete one of the 322 instrumental scenario. To simplify the representation cliques are represented with the bold lines in the figure.

Going to  $l \geq 3$  we see that there might be a quantum violation, since the associated graph has as a subset a  $C_5$  cyclic graph, i.e. the pentagon depicted in fig. 4 that is exactly the Bonet's inequality (4). For cyclic graphs it is known that  $\alpha(C_n) = \lfloor n/2 \rfloor$  and  $\theta(C_n) = n \cos(\pi/n) / (1 + \cos(\pi/n))$ . For  $n = 5$ , it follows directly the gap between the classical and quantum theories, since the classical limit is given by  $\alpha(C_5) = 2$  and the quantum bound is given by  $\theta(C_5) = \sqrt{5}$ .

In this framework, Eq. (4) seems analogous to the KCBS contextual inequality [11]. The difference here is that we are in a bipartite scenario and the real quantum limit is not simply given by the quantity  $\theta(C_5) = \sqrt{5}$ , which constitutes only an upper bound for the maximum achievable quantum violation. To find a tighter bound we can apply the methods described in [10], based on the NPA (Navascues, Pironio, Acin) method [13], which is summarized in the methods section, obtaining the known result for the maximum quantum bound of the Bonet inequality, i.e.  $(3 + \sqrt{2})/2 \approx 2.2071$ .

As shown in the method section below, no other odd an-



ticycle besides  $C_5$  is present for any  $l$ , that is, if we increase the cardinality of the instrumental variable. The first 7-cycle appears as soon as we get to  $n = m = 3$  and  $l = 4$ . This Bonet-like inequality for the instrumental scenario can be written as:

$$P(00|2) + P(02|3) + P(00|0) + P(12|0) + \\ + P(10|1) + P(21|1) + P(22|2) \leq 3 \quad (13)$$

Applying the method cited above for this inequality gives a quantum upper bound of  $q = 3.4142$  at the second order of the NPA hierarchy, which indicates the possibility of a quantum violation. Similarly numerical analysis shows that odd cycle subgraphs with higher number of vertices appear only if we increase the number of possible settings  $l$  while also increasing  $m$ , so for example 9-cycles start to appear for  $l = 6, m = 3$  and 11-cycles for  $l = 7, m = 4$ .

While cycles are the simplest inequalities showing quantum violation, our method can also be employed for the analysis of different inequalities, that can be devised by clever choices of vertices and weights. For example in the instrumental scenario  $(l, m, n) = (4, 2, 2)$  we can find by inspection the inequalities:

$$P(01|2) + P(11|2) + P(10|3) + P(01|3) + \\ + P(00|0) + P(10|0) + P(11|1) + P(00|1) \leq 3 \quad (14)$$

$$P(10|1) + P(11|0) + P(01|0) + P(00|3) + \\ + P(11|3) + P(10|2) + P(00|2) + P(01|1) \leq 3 \quad (15)$$

These inequalities are interesting, since they are represented by the same exclusivity graph of the notorious CHSH inequality for the Bell scenario (see Fig. 5):

$$P(00|10) + P(11|11) + P(01|20) + P(10|21) + \\ + P(00|00) + P(10|01) + P(01|30) + P(11|31) \leq 3 \quad (16)$$

$$P(01|10) - P(10|11) + P(00|20) + P(11|21) + \\ - P(01|00) + P(11|01) + P(00|30) + P(10|31) \leq 3 \quad (17)$$

A well known generalization of the CHSH inequality are the so called GCLMP [1] inequalities, which are defined for any Bell scenario with 2 settings for  $X$  and  $Y$  and  $d$  outputs for  $A$  and  $B$ , and can be written as:

$$I_d^{\text{CGLMP}} = \sum_{k=0}^{d-1} (d-1-k) S_k \leq 3(d-1) \quad (18)$$

$$\text{where } S_k = P(b+k, b|00) + P(a, a+k+1|10) + P(b$$
  

(19)

$i++i$

Table 1: +Caption text+

where the sums  $a + k, a + k + 1$  and  $b + k$  are modulo  $d$ . Using the exclusivity graph method we can find that actually each of the  $S_k$  is classically constrained by  $\alpha(G_k) = 3$ . This can be shown in general. Indeed the graphs  $G_k$  relative to the  $k$  all share the same structure, represented in Fig. ?? there are four cliques, one for each setting  $x, y \in 0, 1$ , and any vertex in each clique is connected to every other vertex in the adjacent clique, except for one. For example  $b + k, b|00$  is connected to any node belonging to the  $(0, 1)$  and the  $(1, 0)$  cliques, except for  $a, a + k|01$  and  $a', a' + k + 1|10$  where  $b + k = a$  and  $a' + k + 1 = b$ . It is easy then to convince that any maximal independent set cannot contain more than 3 vertices. A summary of  $S_k$  inequalities and their quantum bounds is shown in Table 1.  $\square$

Interestingly, except for the case  $(l, m, n) = (4, 2, 2)$ , inequalities with the same structure do not seem to arise in the instrumental case, which suggests that the apparent similarity between the two scenarios, Bell and the instrumental, only arises at for specific number of inputs and outputs.

## Discussion

## Acknowledgements

We acknowledge support from John Templeton Foundation via the grant Q-CAUSAL n°61084 (the opinions expressed in this publication are those of the authors and do not necessarily the views of the John Templeton Foundation). RC acknowledges the Brazilian ministries MEC and MCTIC, funding agency CNPq (PQ grants No. 307172/2017-1 and No 406574/2018-9 and INCT-IQ) and the Serrapilheira Institute (grant number Serra-1708-15763).

## Methods

## Edge colored multigraph technique for approximating the quantum bound

The Lovasz theta of a graph, despite being efficiently computable, only gives an upper bound to the maximal quantum bound, since it ignores the additional constraint deriving from the presence of different parties. To obtain an approximation of this quantity we follow the technique presented in [10]. This method consists in introducing an edge coloring on the exclusivity graph that encodes the information of the party by which the exclusiv-

ity constraints are satisfied. This effectively corresponds to constructing an exclusivity graph  $G_i$  for each party, the resulting object is called a *multigraph*. Having defined a multigraph  $G = G_1, \dots, G_n$  for a given scenario the quantum bound is defined by the quantity:

$$\vartheta(G) = \max_v \sum_{i \in V} |v \cdot a_i^1 \otimes \dots \otimes a_i^n|^2 \quad (20)$$

where  $\{a_i^j\}$  is an orthonormal labelling for  $G_j$  and  $V$  is the set of vertices of  $G$ . This quantity, which can be seen as a generalization of the Lovász theta, is in general not efficiently computable, but can be arbitrarily approximated by a hierarchy of semi-definite programs as described in [10]. In the case of the pentagon in the instrumental scenario we have two colors, and thus two graphs  $G_A$  and  $G_B$ , corresponding to party  $A$  and  $B$  respectively, as shown in Fig. 6. Applying the technique described above to this scenario yields a quantum bound of 2.2071, compatible with the known value for the quantum bound of the Bonet inequality of  $(3 + \sqrt{2})/2$ .

#### **There are no quantum violation for instrumental scenarios with $l = 2$ settings.**

Here we prove that no quantum violation is possible for instrumental scenario with  $l = 2$  possible settings for the instrumental variable  $X$ . This reduces to proving that there are no odd  $n$ -cycles nor  $n$ -anticycles as induced subgraphs in the corresponding exclusivity graph, with  $n \geq 5$ . To see this we can notice that any such graph is composed by two cliques (see for example Fig. 7), corresponding to the events with  $x = 0$  and  $x = 1$ . Any  $n$ -cycle with at least 5 vertices must then have at least 3 mutually connected vertices belonging to the same  $x$ , so they can never form a cycle-graph. Similarly we can show that there cannot be any induced odd anticycle with 5 or more vertices.

#### **There are no cycles $C_n$ with $n \geq 7$ in the $l22$ instrumental scenario.**

In the following we prove that there cannot be a odd anticycle with more than 5 vertices in the exclusivity graph associated to an instrumental scenario of the type  $l22$ .

From the exclusivity conditions (12), given two events  $ab|x$  and  $a'b'|x'$ , they are connected by edge if one of these two conditions is true:

1.  $x = x'$ .
2.  $a = a'$  and  $b \neq b'$ .

Suppose we have a cycle  $C_n$  with  $n \geq 7$ , as in fig. 8, and consider that node 2 in this graph corresponds to an

event which we can arbitrarily identify as  $00|0$ . Among its neighbors 1 and 3, one will necessarily need to satisfy rule 2 (they cannot both satisfy rule 1 or the three nodes would be a clique). So without loss of generality we can assign the event  $01|1$  to 3. Since nodes 5, 6, 7 must not satisfy rule 2 with both 2 and 3, then they must have  $a = 1$ . Moreover 7 and 5 must have the same  $b$ , different from 6. In the same way 1 must not satisfy rule 2 with 6, 5 and 3, so it needs to have  $a = 0$  and  $b = 1$ . At this point, since we only have values  $\{0, 1\}$  for  $a$ , we cannot avoid node 4 to be linked to one of the nodes 1, 2, 6, 7. Thus, the corresponding graph cannot be a cycle.

## **References**

- [1] J. Pearl, *Causality: models, reasoning, and inference*. Cambridge University Press, (2000).
- [2] J. Pearl, *On the testability of causal models with latent and instrumental variables*, Proceedings of the Eleventh conference on Uncertainty in artificial intelligence. Morgan Kaufmann Publishers Inc. (1995).
- [3] B. Bonet, *Instrumentality tests revisited*, Proceedings of the Seventeenth conference on Uncertainty in artificial intelligence. Morgan Kaufmann Publishers Inc. (2001).
- [4] R. Chaves, G. Carvacho, I. Agresti, V. Di Giulio, L. Aolita, S. Giacomini, F. Sciarrino, *Quantum violation of an instrumental test*, Nature Physics 14.3 291 (2018).
- [5] T. Van Himbeeck, J. B. Brask, S. Pironio, R. Ramanathan, A. B. Sainz, E. Wolfe, *Quantum violations in the Instrumental scenario and their relations to the Bell scenario*,
- [6] P. G. Wright, *The tariff on animal and vegetable oils*, The Macmillan Company, (1928).
- [7] C. W. J. Granger, *Investigating causal relations by econometric models and cross-spectral methods*, Econometrica, 424 (1969).
- [8] N. Cartwright, *Causal Structures in Econometrics: On the Reliability of Economic Models*, Recent Economic Thought Series 42, pp 63-89 (1995). arXiv preprint arXiv:1804.04119 (2018).
- [9] A. Cabello, S. Severini, A. Winter, *Graph-theoretic approach to quantum correlations*, Physical review letters, 112(4), 040401 (2014).
- [10] R. Rabelo, C. Duarte, A. J. López-Tarrida, M. T. Cunha, A. Cabello, A. *Multigraph approach to quantum non-locality*, Journal of Physics A: Mathematical and Theoretical, 47(42), 424021 (2014).

- [11] A. A. Klyachko, M. A. Can, S. Binicioğlu, A. S. Shumovsky. *Simple test for hidden variables in spin-1 systems*. Physical review letters, 101(2), 020403 (2008).
- [12] M. Navascués, Y. Guryanova, M. J. Hoban, & A. Acín, *Almost quantum correlations*. Nature Communications 6, (2015).
- [13] M. Navascués, S. Pironio, & A. Acín, *A convergent hierarchy of semidefinite programs characterizing the set of quantum correlations*. New Journal of Physics 10, 073013 (2008).
- [14] L. Lovász, *An Algorithmic Theory of Numbers, Graphs, and Convexity*. CBMS Regional Conference Series in Applied Mathematics (1986), §3.2.
- [15] M. Chudnovsky, N. Robertson, P. Seymour, & R. Thomas, *The strong perfect graph theorem*. Annals of mathematics, 51-229 (2006).

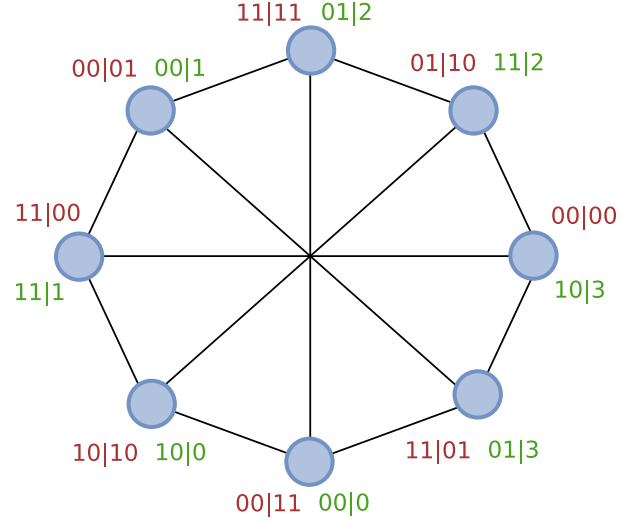


Figure 5: Exclusivity graphs for the the inequality (17) in the Bell scenario (in red) and inequality (15) in the instrumental scenario (in green).

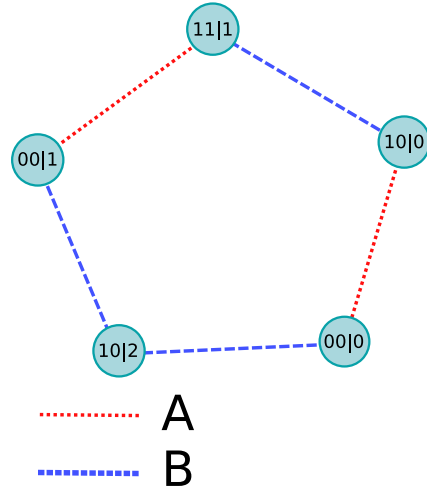


Figure 6: Edge colored exclusivity graph representation of the Bonet inequality. Exclusivity constraints for the party  $A$  and  $B$  are represented by dotted red lines and dashed blue lines respectively.



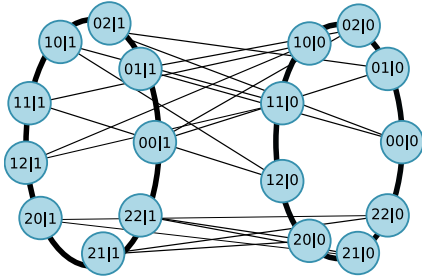


Figure 7: Exclusivity graph for the instrumental scenario 233, showing the impossibility of having cycles with more than 5 vertices. To simplify the figure cliques are represented by bold lines between vertices.

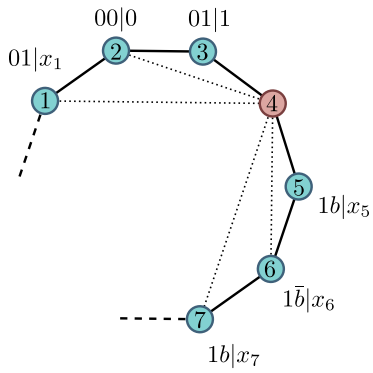


Figure 8: Proof of the impossibility of having cycles with 7 nodes or more in the  $d22$  scenario.